

Josephson current through Anderson insulators

Yasuhiro Asano*

Department of Applied Physics, Hokkaido University, Sapporo 060-8628, Japan

(Received 14 May 2002; published 8 November 2002)

The Josephson effect in superconductor / semiconductor / superconductor junctions is discussed, where semiconductors are in the localization-transport regime. The temperature dependence of the critical Josephson current (J_c) in a single sample is very different from those in other samples. Thus it is impossible to predict the Josephson current in experiments from the ensemble average of the Josephson current in theories. A variety in the temperature-dependence of J_c can be understood by an analysis of the normal conductance near the Fermi energy. In some samples, we find that J_c first increases with decreasing temperatures then decreases in agreement with an recent experiment.

DOI: 10.1103/PhysRevB.66.174506

PACS number(s): 74.80.Fp, 74.25.Fy, 72.10.-d

I. INTRODUCTION

Over the past few decades a considerable number of studies have been made on the dc Josephson effect.^{1,2} In recent years, the Josephson effect has been investigated in superconductor/semiconductor/superconductor (S-Sm-S) junctions, where the Josephson current flows through two-dimensional or quasi-one-dimensional electron systems in semiconductors.³ So far the Josephson effect has been discussed when the normal metal is in the ballistic or the diffusive transport regime.^{1,2} The quasiclassical Green function method, the diagrammatic expansion, and the random matrix theory are useful theoretical tools to study the Josephson current in these transport regimes. In two or quasi-one dimensions, however, a wave function of a quasiparticle is essentially localized owing to the disorder in the system.⁴ Effects of the (Anderson) localization on the Josephson current are expected at very low temperatures. In an experiment, it was found that the amplitude of the critical Josephson current (J_c) first increases with decreasing temperatures, then decreases in S-Sm-S junctions.^{5,6} At present, there is no reasonable explanation for this nonmonotonic temperature dependence of the Josephson current. The Josephson current in the localization regime was also observed in another experiment,⁷ where the indium-oxide thin films were the Anderson insulators. In general, it is difficult to study analytically the Josephson current through the Anderson insulators in the strong localization regime.

In this paper, we study the Josephson current in S-Sm-S junctions by using the recursive Green function method.^{8,9} The Josephson current can be numerically calculated in an arbitrary degree of disorder in semiconductors; this is an advantage of the recursive Green function method. When semiconductors are in the diffusive regime, $\ell \ll L \ll \xi_{AL}$, the ensemble average of J_c increases with decreasing temperatures,¹ where $2\xi_{AL}$ is the localization length of a wave function at the Fermi energy, L is the length of the semiconductors, and ℓ is the elastic mean free path of a quasiparticle. It is known that J_c is proportional to e^{-L/ξ_D} in high temperatures, where $\xi_D \equiv \sqrt{D_0/2\pi T}$ is the coherence length, T is the temperature and D_0 is the diffusion constant in semiconductors. In the localization regime $\xi_{AL} \ll L$, our numerical results show that the ensemble average of $\ln(J_c)$ is

proportional to $-L/\xi_{JC}$ with $\xi_{JC} = \min(\xi_{AL}, \xi_D)$. The dependence of J_c on temperatures in a single sample is, however, very different from those in other samples. We find three typical behaviors of the Josephson current. A variety in the temperature dependence of J_c can be understood by analyzing the normal conductance near the Fermi energy. In the localization regime, the normal conductance in a single sample (G_N) has irregular peak structures when we plot G_N as a function of the Fermi energy. At these resonant peaks, the transmission probability of semiconductors is of the order of unity. In off-resonant states between these peaks, the transmission probability is almost zero. When the Fermi energy is in the resonant peaks or far from any resonant peaks, J_c monotonically increases with decreasing T . Conversely, when the Fermi energy is near the resonant peaks but still in the off-resonant states, J_c first increases with decreasing temperatures then decreases. We think that the reentrant behavior in our simulation corresponds to that found in the experiment.⁵ Throughout this paper, we take units of $\hbar = k_B = 1$.

This paper is organized as follows. In Sec. II, we explain the theoretical model and the method of numerical simulation. Numerical results of the Josephson current are shown in Sec. III. The discussion is given in Sec. IV. We summarize this paper in Sec. V.

II. MODEL AND METHOD

Let us consider the S-Sm-S junction on the quasi-one-dimensional tight-binding lattice as shown in Fig. 1, where (j, m) labels the lattice site, and W is the number of lattice

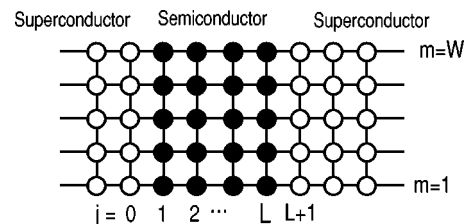


FIG. 1. The S-Sm-S junction is illustrated. The circles denote the lattice sites. The system consists of the semiconductor (filled circles) and two superconducting lead wires (open circles).

sites in the transverse direction. The lattice sites for $1 \leq j \leq L$ represent the semiconductor (filled circles). The perfect superconducting lead wires are attached to both sides of the semiconductor for $-\infty \leq j \leq 0$ and $L+1 \leq j \leq \infty$ (open circles). The BCS Hamiltonian leads to

$$H_{\text{BCS}} = -t \sum_{j,m,\sigma} [c_{j+1,m,\sigma}^\dagger c_{j,m,\sigma} + c_{j,m+1,\sigma}^\dagger c_{j,m,\sigma} + \text{H.c.}] \\ + \sum_{j,m,\sigma} [(\epsilon_{j,m} + 4t - \mu_F) c_{j,m,\sigma}^\dagger c_{j,m,\sigma}] \\ - \sum_{j,m} [\Delta_{j,m} c_{j,m,\downarrow}^\dagger c_{j,m,\uparrow}^\dagger + \text{H.c.}], \quad (1)$$

where $c_{j,m,\sigma}^\dagger$ ($c_{j,m,\sigma}$) is the creation (annihilation) operator of an electron at (j,m) with spin $\sigma = \uparrow$ or \downarrow , and $\Delta_{j,m} = |\Delta_{j,m}| e^{i\varphi_{j,m}}$ is the pair potential. We assume that $\Delta_{j,m} = \Delta e^{i\varphi_L}$ for $j \leq 0$, $\Delta_{j,m} = 0$ for $1 \leq j \leq L$, and $\Delta_{j,m} = \Delta e^{i\varphi_R}$ for $j \geq L+1$. The dependence of Δ on temperatures is described by the BCS theory. The critical temperature is $T_c \approx 0.57\Delta_0$, where Δ_0 is the amplitude of the pair potential at the zero temperature. The random on-site potential is denoted by $\epsilon_{j,m}$, which is given randomly in the range of $-V/2 \leq \epsilon_{j,m} \leq V/2$ for $1 \leq j \leq L$. In what follows, we measure the energy in units of the hopping integral denoted by t from the chemical potential of junctions. The Fermi energy μ_F corresponds to the difference in energy between the band edge and the chemical potential. The length is measured in units of the lattice constant denoted by a_0 . Throughout this paper, we fix $W=20$, $\mu_F=2.0t$, $V=3.0t$, and $\Delta_0=0.01t$. In semiconductors, the number of propagating channels at the Fermi energy is 10 in these parameters.

The BCS Hamiltonian is diagonalized by the Bogoliubov transformation

$$\begin{bmatrix} c_{j,m,\uparrow} \\ c_{j,m,\downarrow}^\dagger \end{bmatrix} = \sum_{\nu} \begin{bmatrix} u_{\nu}(j,m) & -v_{\nu}^*(j,m) \\ v_{\nu}(j,m) & u_{\nu}^*(j,m) \end{bmatrix} \begin{bmatrix} \gamma_{\nu,\uparrow} \\ \gamma_{\nu,\downarrow}^\dagger \end{bmatrix}, \quad (2)$$

where u_{ν} and v_{ν} are the wave functions of a quasiparticle which satisfy the Bogoliubov-de Gennes (BdG) equation.¹⁰ To solve the BdG equation, we apply the recursive Green function method⁹ and calculate the Matsubara Green function in a matrix form,

$$\check{G}_{\omega_n}(j,j') = \sum_{\nu} \frac{\Psi_{\nu}(j)\Psi_{\nu}^\dagger(j')}{i\omega_n - E_{\nu}}, \quad (3)$$

where $\omega_n = (2n+1)\pi T$ is the Matsubara frequency. The wave function $\Psi_{\nu}(j)$ has $2W$ components, and the m th [(the $(m+W)$ th)] element is $u_{\nu}(j,m)$ [$v_{\nu}(j,m)$]. The Josephson current in semiconductors ($1 < j < L$), is given by⁹

$$J(j) = -ieT \sum_{\omega_n} t \text{Tr}[\check{G}_{\omega_n}(j+1,j) - \check{G}_{\omega_n}(j,j+1)]. \quad (4)$$

We note that $J(j)$ is independent of j when we consider the direct-current Josephson effect.

In a conventional way for calculating the Josephson current, we first estimate the energy of the Andreev bound states

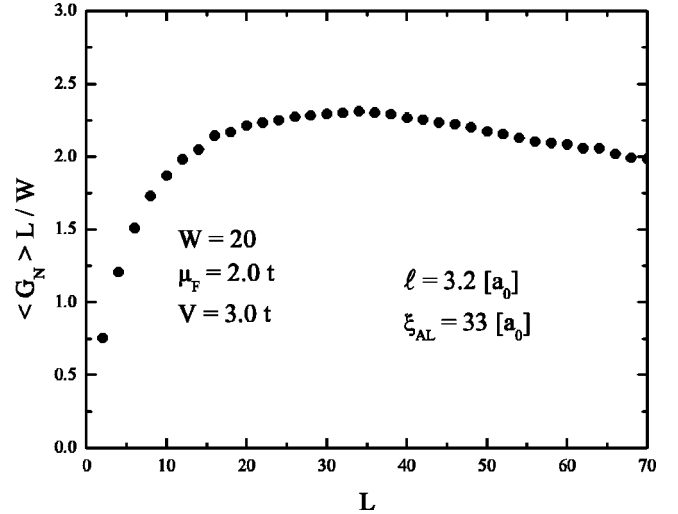


FIG. 2. The normal conductance is plotted as a function of L , where $W=20$, $\mu_F=2t$, and $V=3t$. The vertical axis is $\langle G_N \rangle L/W$ which corresponds to the conductivity when the normal metals are in the diffusive regime.

of the junction. Then the Josephson current is given by the derivative of the energy with respect to the phase-difference between two superconductors. In 1991, Furusaki and Tsukada established an alternative method,¹¹ where the Josephson current is described by the two Andreev reflection¹² coefficients. These two methods yield exactly the same Josephson current even though the way of calculation are different from each other. Furusaki and Tsukada also showed a relation between the Josephson current and the space-derivative of the Matsubara Green function which is shown in Eq. (4). We note here that Eq. (4) is a useful expression when we numerically calculate the Josephson current by using the lattice-Green function method. The details of the simulation are given in Ref. 9.

III. RESULT

We numerically calculate the normal conductance (G_N) at $T=0$ by using the conventional recursive Green function method,⁸ where the two superconductors in Fig. 1 are replaced by perfect normal lead wires and the last term in Eq. (1) is deleted. In Fig. 2, we show the normal conductance as a function of L . The results are averaged over a number of samples with different impurity configurations. The ensemble averaged values are denoted by $\langle \dots \rangle$. The vertical axis indicates $\langle G_N \rangle L/W$, which becomes the conductivity when the disordered region is in the diffusive transport regime. When the disordered region is in the quasiballistic transport regime, $\langle G_N \rangle \sim W$. Thus $\langle G_N \rangle L/W$ is proportional to L , as shown for $0 < L < 10$. When the disordered region is in the diffusive regime as shown in $20 < L < 50$, $\langle G_N \rangle L/W$ is independent of L because the conductivity is independent of the sample size. When the disordered region is in the localization regime, $\langle G_N \rangle L/W$ is proportional to $\exp(-L/\xi_{\text{AL}})$ for large L . From the numerical results in the diffusive regime, we estimate the mean free path ($\ell \sim 3.2a_0$) and the diffusion constant (D_0) by a relation $(L/W)\langle G_N \rangle = e^2 N_F D_0$, where

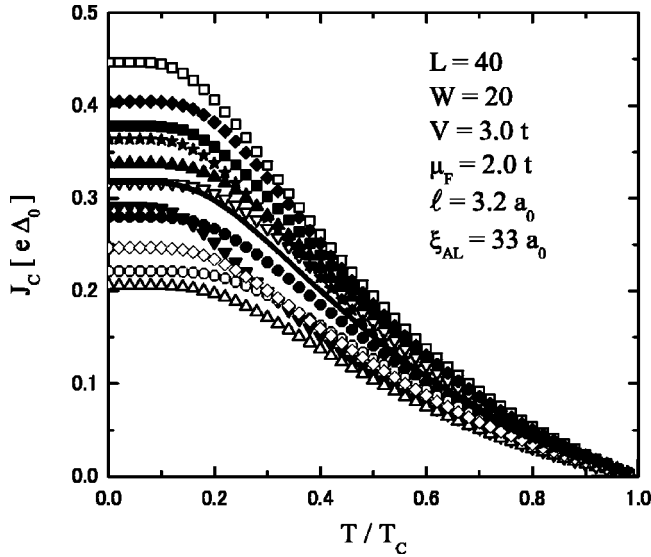


FIG. 3. The Josephson current in the diffusive regime is shown for several samples with different configurations of impurities, where $L=40$. The solid line is the ensemble average of the Josephson current.

N_F is the density of states at the Fermi energy. From numerical results for $L \gg \xi_{AL}$, we also estimate the localization length (ξ_{AL}) is about $33a_0$ by assuming a relation $\langle \ln G_N \rangle \propto -L/\xi_{AL}$. We note that ξ_{AL} depends on parameters such as μ_F and V .

For comparison, we first show numerical results of the Josephson current in the diffusive regime. When semiconductors are in the diffusive transport regime, the ensemble average of the critical Josephson current is given by^{1,13}

$$\langle J_c \rangle = J_0 2 \frac{\Delta}{\Delta_0} T \sum_{\omega_n} \frac{\Delta}{\omega_n^2 + \Delta^2} \frac{\eta_n}{\sinh \eta_n}, \quad (5)$$

$$J_0 = \frac{\pi \Delta_0}{2e \langle R_N \rangle}, \quad (6)$$

$$\eta_n = \sqrt{2n+1} \frac{L}{\xi_D}, \quad (7)$$

where $\langle R_N \rangle$ is the normal resistance of semiconductors. We note that $\langle J_c \rangle$ is proportional to e^{-L/ξ_D} in high temperatures.

In Fig. 3, we show the critical Josephson current as a function of temperatures for several samples with different random impurity configurations, where $L=40$, and we fix the phase difference $\delta\varphi = \varphi_L - \varphi_R$ at $\pi/2$. There are finite sample-to-sample fluctuations in J_c ,^{14,15} but the Josephson current in a single sample is well described by $\langle J_c \rangle$ which is denoted by the solid line and is well explained by the analytical expression in Eq. (5). In recent papers,¹⁶⁻¹⁸ it was pointed out that Eq. (5) is not correct in low temperatures and the nonsinusoidal current-phase relation is observed. As a result, the Josephson current takes its maximum at $\delta\varphi > \pi/2$. In this paper, we approximately use Eq. (5) because the purpose of this paragraph is to confirm the two characteristic features of the Josephson current in the diffusive re-

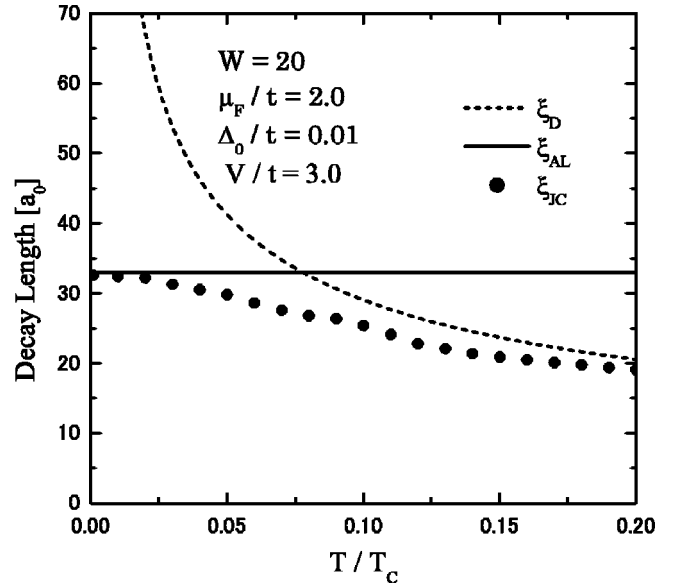


FIG. 4. The decay length of the Josephson current (ξ_{JC}) is compared with the localization length of the normal current (ξ_{AL}) and the coherence length (ξ_D) in the diffusive regime.

gime, i.e., (i) J_c monotonically increases with decreasing T , and (ii) J_c in a specific sample is well described by $\langle J_c \rangle$.

When semiconductors are in the localization regime, J_c is expected to be proportional to $e^{-L/\xi_{JC}}$, where ξ_{JC} is the decay length of the Josephson current. In Fig. 4, we compare ξ_{JC} with ξ_D and ξ_{AL} . The decay length ξ_{JC} is estimated from the critical current by using a relation $\langle \ln J_c \rangle \propto -L/\xi_{JC}$ in the limit of $L \gg \xi_{JC}$. The localization length at $T=0$ is plotted with the solid line. These decay length are ensemble averaged values, but we omit $\langle \dots \rangle$ for simplicity.

The numerical results show that $\xi_{JC} \sim \xi_D$ in high temperatures and ξ_{JC} approaches to ξ_{AL} in the limit of the zero-temperature. Thus we conclude that $\xi_{JC} = \min(\xi_{AL}, \xi_D)$. We define T_0 by an equation

$$\xi_{AL} = \xi_D |_{T=T_0}, \quad (8)$$

and it is about $0.075T_c$ in Fig. 4. Effects of the localization on the Josephson current are expected at low temperatures for $T < T_0$.

In the localization regime, the sample-to-sample fluctuations of the conductance (δG_N) becomes larger than $\langle G_N \rangle$ itself. In the Josephson current, fluctuations (δJ_c) are also larger than $\langle J_c \rangle$. However, the logarithm of the conductance and that of the Josephson current are self-averaged values. Thus ξ_{AL} and ξ_{JC} are larger than their fluctuations. In Fig. 4, therefore, we calculate logarithm of the transport properties such as $\langle \ln(G_N) \rangle$ and $\langle \ln(J_c) \rangle$.

From numerical results, we show $\exp(\langle \ln J_c \rangle)$ in Fig. 5, where $L=300$. The calculated results increase monotonically with decreasing temperatures. It may be possible to consider that $\exp(\langle \ln J_c \rangle)$ reflects some averaged behavior of the Josephson current in the localization regime. However, characteristic behaviors of the Josephson current in a single sample are very different from $\exp(\langle \ln J_c \rangle)$ in Fig. 5. In Figs. 6(a)–

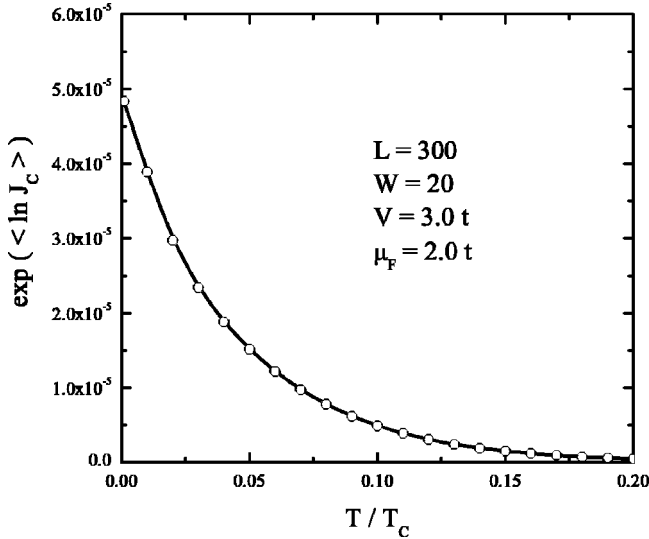


FIG. 5. $\exp(\langle \ln J_c \rangle)$ is shown as a function of temperatures, where $L=300$.

6(c) we show the Josephson current as a function of temperatures for several samples. Scales of the vertical axis in (a), (b) and (c) are different order in magnitude although degree of randomness in semiconductors are the same for all samples: which arises the large fluctuations in the Josephson current. We find three typical temperature-dependence of J_c in Fig. 6: (i) J_c increases with decreasing T then saturates in low temperatures, (ii) J_c shows no saturation even in low temperatures, and (iii) J_c first increases with decreasing T then decreases. We believe that the reentrant behavior in (iii) corresponds to that observed in the experiment.⁵

The electronic states near the Fermi energy are responsible for a variety in the temperature-dependence of J_c in the localization regime. To make this point clear, we plot the normal conductance in a single sample as a function of the Fermi energy in Fig. 7, where $L=300$. The Fermi energy is given by $\mu_F = 2.0t + \delta\mu_F$. There are number of irregular conductance peaks. The electronic states at these peaks are characterized by a relatively large localization length and the transmission probabilities have large values of the order of unity. Thus these peaks are understood in terms of the resonant transmission peaks. Conversely, the transmission probabilities are very small in off-resonant states between these conductance peaks. The peak structures are a typical behavior of the conductance in the localization regime and reflect the sample-specific impurity configuration.

In Fig. 8, we show typical temperature dependences of the Josephson current in three samples with $L=300$. In the insets, the normal conductance in these samples is plotted as a function of the Fermi energy, where a vertical broken line indicates $\mu_F = 2.0t$.

When the Fermi energy is in off-resonant states, the Josephson current increases with decreasing temperatures for $T/T_c > 0.03$ as shown in Fig. 8(a). In low temperatures for $T/T_c < 0.03$, J_c saturates. This saturation in very low temperatures is one of the characteristic behavior of J_c in localization regime. Actually $0.03T_c$ is close to $T_0 = 0.075T_c$ in Eq. (8). It is known that the critical current in

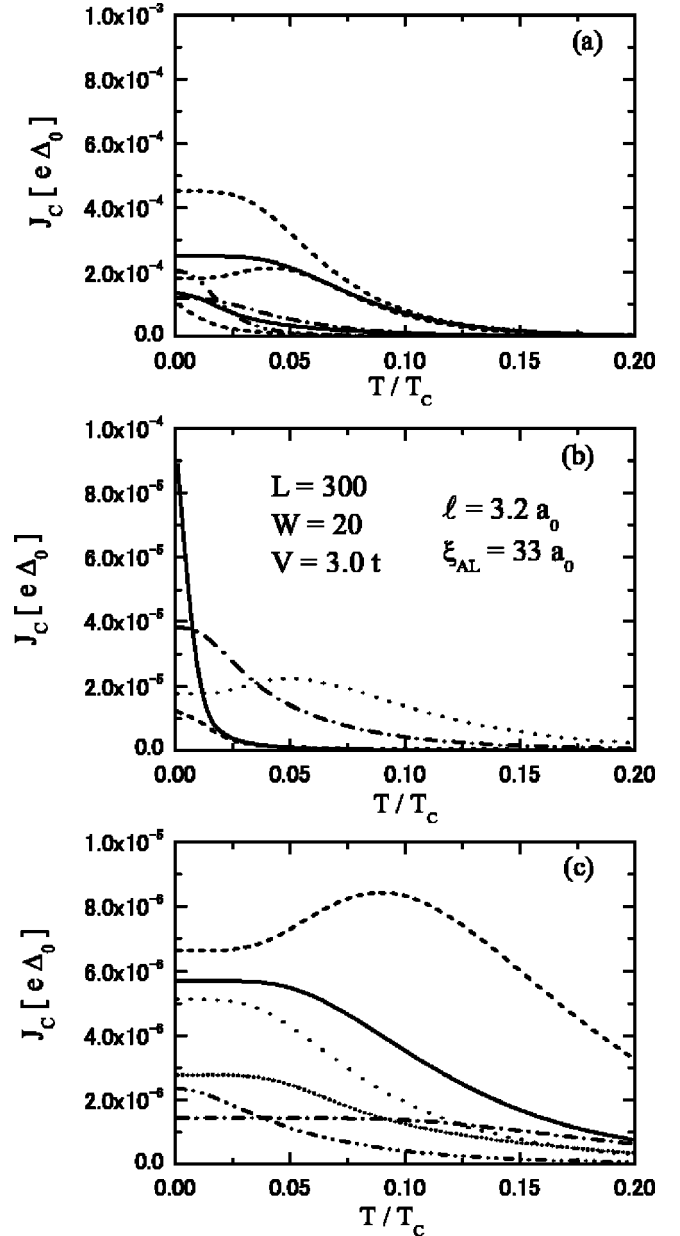


FIG. 6. The Josephson current for several samples are shown as a function of temperatures, where $L=300$.

superconductor/insulator/superconductor (SIS) junctions¹⁹ saturates in low temperatures. The current expression in SIS is given by

$$J_c = J_0 2 \frac{\Delta}{\Delta_0} T \sum_{\omega_n} \frac{\Delta}{\omega_n^2 + \Delta^2}, \quad (9)$$

$$= J_0 \frac{\Delta}{\Delta_0} \tanh\left(\frac{\Delta}{2T}\right). \quad (10)$$

In SIS systems, we implicitly assume that the coherence length is always longer than the thickness of the insulators. The essential difference between Eqs. (5) and (9) is the coherence factor in normal metals $\eta_n / \sinh \eta_n$ in Eq. (5) which limits the region of the phase-coherent transport at finite temperatures. The Andreev reflection at junction interfaces arises

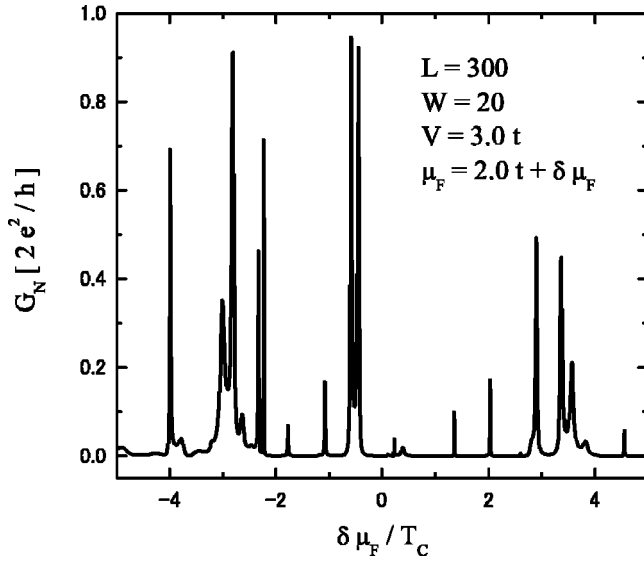


FIG. 7. The normal conductance in a single sample is plotted as a function of the Fermi energy around $\mu_F = 2.0t$, where $L = 300$.

the common factor $\Delta^2/(\omega_n^2 + \Delta^2)$.²⁰ In the diffusive regime, the coherence factor increases with decreasing T , which characterizes the dependence of $\langle J_c \rangle$ on temperatures. At $T = 0$, the coherence factor becomes unity, which means that a quasiparticle can travel all over the normal metal without losing the phase coherence. In the localization regime, it is reasonable to consider that some coherence factor $[F(\omega_n)]$ describes the spatial region of the phase-coherent propagation. Although we cannot give a microscopic expression of $F(\omega_n)$, the Josephson current may be described by an equation

$$J_c \propto T \sum_{\omega_n} \frac{\Delta}{\omega_n^2 + \Delta^2} F(\omega_n). \quad (11)$$

In high temperatures for $T > T_0$, F may increase with decreasing temperature. However, for $T < T_0$, F must be a constant independent of temperatures because the motion of a quasiparticle is limited within the localization length. As a consequence, the current expression is equivalent to Eq. (9) which leads to the saturation of J_c in low temperatures.

When the Fermi energy is in one of resonant peaks as shown in Fig. 8(b), J_c monotonically increases with T . This is a typical behavior of the resonant transmission in low temperatures. We do not have to consider coherence factors in this case because the resonant peak itself is a result of the phase-coherence of a quasiparticle.

The most interesting behavior of J_c in the localization regime is shown in Fig. 8(c), where the Fermi energy is close to one of the resonant peaks but still in the off-resonant states as shown in the inset. When temperatures are higher than the difference between the Fermi energy and the resonant peak, the resonant states can contribute to the Josephson current. The resonant states, however, cannot contribute to the current when the temperatures are lower than the difference between the Fermi energy and the resonant peak. This explains

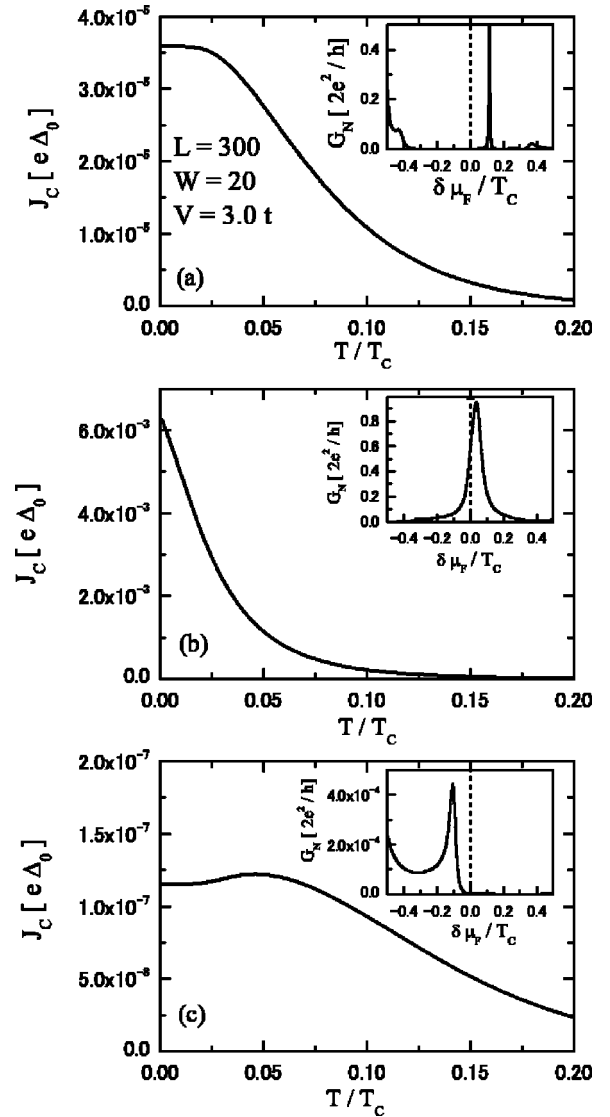


FIG. 8. A typical temperature dependence of the Josephson current is shown, where $L = 300$. In insets, the normal conductance is plotted as a function of the Fermi energy. In (a), the Fermi energy is in off-resonant states. The Fermi energy is in one of resonant peaks in (b). The Fermi energy is close to a resonant peak in (c).

the reentrant behavior of J_c in (c). Since the Fermi energy is at the off-resonant states, J_c saturates in low temperatures. In the experiment,⁵ the reentrant behavior of J_c was reported. The calculated results indicate that the resonant states in the Anderson insulators is one of possible candidate to explain the experimental results of J_c .

IV. DISCUSSION

At finite temperatures, variable range hopping²¹ (VRH) dominates the temperature-dependence of the conductance in the strong localization regime. In this paper, the Josephson current stemming from VRH is not taken into account. We think, however, that such inelastic propagating processes do

not contribute to the Josephson current because a quasiparticle loses its phase memory while VRH occurs.

When semiconductors are in the diffusive regime, $\langle J_c \rangle$ means the expected values of experimental measurements in a single sample. On the other hand, in the localization regime, the characteristic behavior of the Josephson current in a single sample depend strongly on microscopic information of the sample such as the impurity configuration. As a result, $\langle J_c \rangle$ does not predict any experiments for a single sample. We note here that we reach almost the same conclusion when the diffusive normal metal is sandwiched between two anisotropic superconductors.²⁰ In these systems, $\langle J_c \rangle$ vanishes for all temperatures when a node plane of the pair potential is perpendicular to the junction interface.²² However, the Josephson current in a single sample remains a finite value.¹³ Since the Josephson current is a result of the phase coherence of a quasiparticle, $\langle J_c \rangle$ sometimes loses its physical meaning.

In this paper, we assume *s*-wave superconductors. In the case of anisotropic superconductors, effects of zero-energy-states^{23–25} on the Josephson current in the localization regime may be an important problem. We have already developed the method of the numerical simulation in *d*-wave superconductors.²⁶ This issue will be addressed, and results will be given elsewhere.

V. CONCLUSION

We have studied the dc Josephson effect in S-Sm-S junctions, where semiconductors are in the localization-transport regime. The Josephson current is numerically calculated by using the lattice recursive Green function method. The decay length of the ensemble averaged Josephson current is given by the coherence length for high temperatures. In low temperatures, the decay length approaches the localization length of the normal conductance. The ensemble averaged values, however, cannot explain the characteristic behavior of the Josephson current in a single sample because the Josephson current is a result of the phase coherence of a quasiparticle. The temperature dependence of the Josephson current in a single sample is very different from that in other samples. The variety in the temperature dependence of J_c can be explained by analyzing the normal conductance near the Fermi energy. When the Fermi energy is near a resonant conductance peak, J_c first increases with decreasing temperatures then decreases. This reentrant behavior in J_c is consistent with that observed in an experiment.

ACKNOWLEDGMENTS

The author is indebted to H. Akera, T. Ohtsuki, Y. Tanaka, J. Nitta, and G. E. W. Bauer for useful discussion.

*Electronic address: asano@eng.hokudai.ac.jp

¹K.K. Likharev, Rev. Mod. Phys. **51**, 101 (1979).

²Y. Imry, *Introduction to Mesoscopic Physics* (Oxford University Press, New York, 1997), Chap. 7.

³B. J. van Wees and H. Takayanagi, in *Mesoscopic Electron Transport*, Vol. 345 of *NATO Advanced Study Institute, Series E: Applied Sciences*, edited by L. L. Sohn, L. P. Kouwenhoven, and G. Schön (Kluwer, Dordrecht, 1996).

⁴E. Abrahams, P.W. Anderson, D.C. Licciardello, and T.V. Ramakrishnan, Phys. Rev. Lett. **42**, 673 (1979).

⁵H. Takayanagi, J.B. Hansen, and J. Nitta, Phys. Rev. Lett. **74**, 162 (1995).

⁶H. Takayanagi and T. Akazaki, Solid State Commun. **96**, 815 (1995).

⁷A. Frydman and Z. Ovadyahu, Phys. Rev. B **55**, 9047 (1997).

⁸P.A. Lee and D.S. Fisher, Phys. Rev. Lett. **47**, 882 (1981).

⁹A. Furusaki, Physica B **203**, 214 (1994).

¹⁰P. G. de Gennes, *Superconductivity of Metals and Alloys* (Benjamin, New York, 1966).

¹¹A. Furusaki and M. Tsukada, Solid State Commun. **78**, 299 (1991).

¹²A.F. Andreev, Zh. Éksp. Teor. Fiz. **46**, 1823 (1964) [Sov. Phys.

JETP **19**, 1228 (1964)].

¹³Y. Asano, Phys. Rev. B **64**, 014511 (2001).

¹⁴B.I. Altshuler and B.Z. Spivak, Zh. Éksp. Teor. Fiz. **93**, 609 (1987) [Sov. Phys. JETP **65**, 343 (1987)].

¹⁵C.W.J. Beenakker, Phys. Rev. Lett. **67**, 3836 (1991).

¹⁶P. Dubos, H. Courtois, B. Pannetier, F.K. Wilhelm, A.D. Zaikin, and G. Schön, Phys. Rev. B **63**, 064502 (2001).

¹⁷A.D. Zaikin and G.F. Zharkov, Fiz. Nizk. Temp. **7**, 375 (1981) [Sov. J. Low Temp. Phys. **7**, 184 (1981)].

¹⁸F.K. Wilhelm, A.D. Zaikin and G. Shön, J. Low Temp. Phys. **106**, 305 (1997).

¹⁹V. Ambegaokar and A. Baratoff, Phys. Rev. Lett. **10**, 486 (1963); **11**, 104 (1963).

²⁰Y. Asano, Phys. Rev. B **64**, 224515 (2001).

²¹N. Mott, *Metal-Insulator Transitions*, 2nd ed. (Taylor and Francis, London, 1990).

²²Y. Asano, J. Phys. Soc. Jpn. **71**, 905 (2002).

²³Y. Tanaka and S. Kashiwaya, Phys. Rev. Lett. **74**, 3451 (1995).

²⁴Y. Tanaka and S. Kashiwaya, Phys. Rev. B **53**, R11 957 (1996).

²⁵Y.S. Barash, H. Burkhardt, and D. Rainer, Phys. Rev. Lett. **77**, 4070 (1996).

²⁶Y. Asano, Phys. Rev. B **63**, 052512 (2001).